INTERNATIONAL JOURNAL FOR NUMERICAL METHODS IN FLUIDS
Int. J. Numer. Meth. Fluids 2007; **54**:1269–1290
Published online 16 January 2007 in Wiley InterScience (www.interscience.wiley.com). DOI: 10.1002/fld.1418

Application of second-order adjoint technique for conduit flow problem

T. Kurahashi*,† and M. Kawahara‡

Department of Civil Engineering, Chuo University, Kasuga 1-13-27, Bunkyo-ku, Tokyo 112-8551, Japan

SUMMARY

This paper presents the way to obtain the Newton gradient by using a traction given by the perturbation for the Lagrange multiplier. Conventionally, the second-order adjoint model using the Hessian/vector products expressed by the product of the Hessian matrix and the perturbation of the design variables has been researched (*Comput. Optim. Appl.* 1995; **4**:241–262). However, in case that the boundary value would like to be obtained, this model cannot be applied directly. Therefore, the conventional second-order adjoint technique is extended to the boundary value determination problem and the second-order adjoint technique is applied to the conduit flow problem in this paper. As the minimization technique, the Newton-based method is employed. The Broyden–Fletcher–Goldfarb–Shanno (BFGS) method is applied to calculate the Hessian matrix which is used in the Newton-based method and a traction given by the perturbation for the Lagrange multiplier is used in the BFGS method. Copyright © 2007 John Wiley & Sons, Ltd.

Received 9 August 2006; Revised 3 November 2006; Accepted 10 November 2006

KEY WORDS: second-order adjoint technique; Newton gradient; traction of perturbation for Lagrange multiplier; BFGS method; Newton-based method; finite-element method

1. INTRODUCTION

Of late, flood damage has been occurring frequently in urban areas. The purposes of sewage are the maintenance of water quality, the improvement of living environment and the exclusion of stormwater. A measure for stormwater is one of the important roles of the sewer. Storm tends to occur frequently by abnormal weather or activation of a front by a typhoon. Therefore, to prevent the flood damage, the countermeasure for stormwater is an urgent business. Recently, introduction

*Correspondence to: T. Kurahashi, Department of Civil Engineering, Chuo University, Kasuga 1-13-27, Bunkyou-ku, Tokyo 112-8551, Japan.
†E-mail: tkura@civil.chuo-u.ac.jp
‡E-mail: kawa@civil.chuo-u.ac.jp

of the flood control system is considered as one of the countermeasures for stormwater. In case that the flood control system is constructed, it is desired that many examinations are carried out based on the control theory and the flood control system is adequately operated.

Thus, in case that the design variables are determined based on the control theory, a performance function is defined as the performance index. This control problem can be expressed by the minimization problem of the performance function, and the problem is formulated under the constraint conditions that can be expressed by the state equation, the initial and boundary conditions. In general, the gradient-based method [1, 2] or the Newton-based method is employed for minimizing the performance function. In this study, we focus on the Newton-based method that is well known as the method that is used to obtain the first convergence rate. It is necessary that the information of the Hessian matrix is obtained in case that the Newton-based method is employed [3–5]. Conventionally, the second-order adjoint model using the Hessian/vector products expressed by the product of the Hessian matrix and the perturbation of the design variables has been researched [6–9]. This model was developed for the initial value determination problem, and this model cannot be directly applied to the boundary value determination problem. Because the gradient vector of the performance function with respect to the boundary value is expressed by the traction vector for adjoint equation, though that of the performance function with respect to the initial value is expressed by the adjoint variable itself. Therefore, the second-order adjoint technique for the boundary value determination problem is developed; this technique was applied to the heat transfer control problem [10]. Consequently, if the second-order adjoint technique is applied to that problem, fast convergence rate could be obtained in comparison with the first-order adjoint technique. The purpose of this study is to apply the second-order adjoint technique for the boundary value determination problem in the conduit flow, and the verification of the effect by using this technique and the application of this technique for a flood control problem are carried out. To compute the state equation and adjoint equation, the finite-element method is employed. As the numerical experiments, to verify the propriety of the second-order adjoint technique, a simple conduit flow problem is used. After that, this technique is applied to the flood control problem.

2. FORMULATIONS

2.1. First variation

To express the flow behaviour in a conduit, the Saint–Venant equation is frequently employed. The Saint–Venant equation is written as

$$\dot{Q} + (QV)_{,x} + gA(\cos\theta)h_{,x} - g(s_0 A - fQ) = 0 \quad \text{in } Lt \in [t_0, t_f] \tag{1}$$

$$\dot{A} + Q_{,x} = 0 \quad \text{in } Lt \in [t_0, t_f] \tag{2}$$

where x is the longitudinal distance along the channel, t is the time, Q is the flow quantity, A is the cross-section area, V is the water velocity, h is the surface level of the water in the conduit, θ is the angle of the slope, g is the acceleration of gravity, s_0 is the slope of bottom of the conduit, and f is the coefficient of friction and is given by $(n^2 Q/R^{4/3}A)$. n is the Manning coefficient of roughness, R is the hydraulic mean depth, and is given by (A/S). S is the wetted perimeter. The diagram of the conduit flow is shown in Figure 1.

DOI: 10.1002/fld

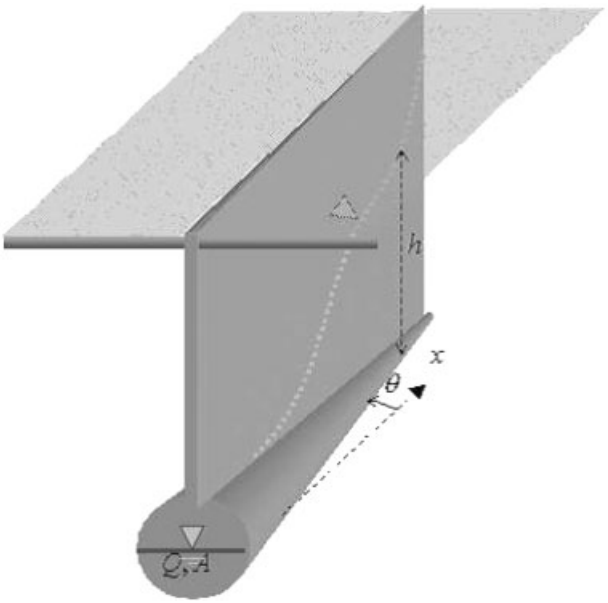

Figure 1. Diagram of conduit flow.

The initial and boundary conditions are written as

$$\begin{aligned} Q(t_0) &= \hat{Q}(t_0) && \text{in } L \\ A(t_0) &= \hat{A}(t_0) && \text{in } L \\ Q(t) &= \hat{Q}(t) && \text{at } X_1, \quad t \in [t_0, t_f] \\ A(t) &= \hat{A}(t) && \text{at } X_1, \quad t \in [t_0, t_f] \\ Q(t) &= Q_{\text{Cont.}}(t) && \text{at } X_{\text{Cont.}}, \quad t \in [t_0, t_f] \end{aligned} \tag{3}$$

where X_1 means the points at which the boundary condition is given and $X_{\text{Cont.}}$ means the points at which the control discharge is given.

To apply the Galerkin method for the spatial discretization of the state equation, the following finite-element equation can be obtained. The Crank–Nicolson scheme is applied to the temporal discretization for the finite-element equation

$$\begin{aligned} &[M]\{\dot{Q}\} + [S(Q),_x]\{V\} + [S(V),_x]\{Q\} + g(\cos\theta)[S(h),_x]\{A\} \\ &-g(s_0[M]\{A\} - f[M]\{Q\}) = \{0\} \end{aligned} \tag{4}$$

$$[M]\{\dot{A}\} + [S,_x]\{Q\} = \{0\} \tag{5}$$

where $[M]$, $[S,_x]$, $[S,_x(Q)]$ and $[S(h),_x]$ mean the coefficient matrices of the finite-element equation. In addition, the Preissmann slot model [11] is included in the analysis of conduit flow.

DOI: 10.1002/fld

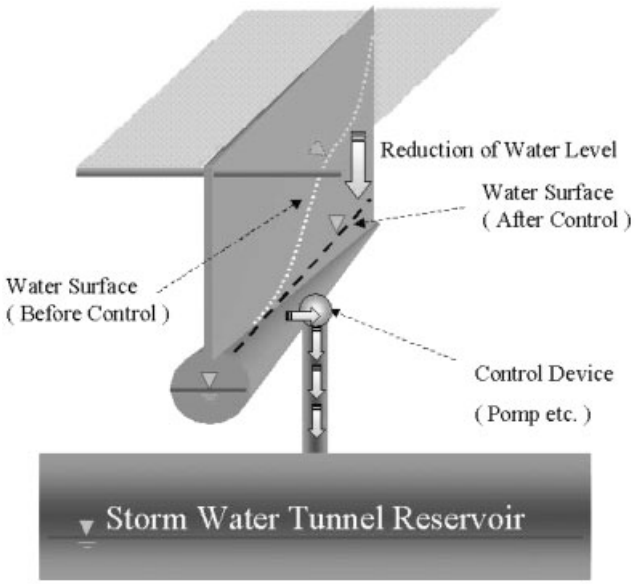

Figure 2. Diagram of flood control system.

In this section, the flood control problem is considered. To prevent the flood damage, the stormwater tunnel reservoir is constructed underground. Here, let us consider a system where the water flow in the conduit is adequately conducted to the stormwater tunnel reservoir by using the control device. The diagram of the flood control system is shown in Figure 2. To solve this problem, the performance function is defined as follows. The first term consists of physical value of the control target and can be denoted by the square form of the residual between the computed water level h and the target water level h_t. The second term means the evaluation term of the control discharge $Q_{\text{Cont.}}$ and can be expressed by the square form of the control discharge:

$$J = \frac{1}{2} \int_{t_0}^{t_f} \sum_{e=1}^{n_{\text{el}}} \{h - h_t\}^{\text{T}} [P] \{h - h_t\} \, \mathrm{d}t \tag{6}$$

where $[P]$ means the weighting diagonal matrix, and n_{el} means the total number of elements. The performance function can be represented by the form of the cross-section area A, because the water level h is the function of cross-section area A. Therefore, the performance function can be denoted as

$$J = \frac{1}{2} \int_{t_0}^{t_f} \sum_{e=1}^{n_{\text{el}}} \{A - A_t\}^{\text{T}} [P] \{A - A_t\} \, \mathrm{d}t \tag{7}$$

The purpose is to find the adequate control discharge $Q_{\text{Cont.}}$ to minimize the performance function J under the constraints of the state equation, the initial and the boundary conditions. The fact that the performance function is minimized means that the computed water level h is as close as the target water level h_{Target}.

The performance function is constrained by the state equation, because the performance function can be expressed by the solution of the state equation. Therefore, the Lagrange multiplier method

DOI: 10.1002/fld

is introduced to the minimization problem with constraint condition. The performance function extended by the Lagrange multipliers and the state equation can be expressed as

$$J^* = J + \int_{t_0}^{t_f} \sum_{e=1}^{n_{\mathrm{el}}} \{\lambda\}^{\mathrm{T}}([M]\{\dot{Q}\} + \{F(Q, A)\}) + \{\mu\}^{\mathrm{T}}([M]\{\dot{A}\} + \{G(Q)\})\,\mathrm{d}t \tag{8}$$

where $\{\lambda\}$ and $\{\mu\}$ are the Lagrange multipliers for the flow quantity $\{Q\}$ and the cross-section area $\{A\}$. $\{F(Q, A)\}$ and $\{G(Q)\}$ mean the steady terms for the momentum and the continuity equations. These functions are written as

$$\begin{aligned}\{F(Q, A)\} = {} & [S(Q)_{,x}]\{V\} + [S(V)_{,x}]\{Q\} + g(\cos\theta)[S(A)_{,x}]\{h\} \\ & - g(s_0[M]\{A\} - f[M]\{Q\})\end{aligned} \tag{9}$$

$$\{G(Q)\} = [S_{,x}]\{Q\} \tag{10}$$

To derive the stationary condition, the first variation of the extended performance function is calculated. Consequently, the following first-order adjoint equation can be obtained:

$$-[M]^{\mathrm{T}}\{\dot{\lambda}\} + \left[\frac{\partial F}{\partial Q}\right]^{\mathrm{T}}\{\lambda\} + \left[\frac{\partial G}{\partial Q}\right]^{\mathrm{T}}\{\mu\} = \{s\} \tag{11}$$

$$-[M]^{\mathrm{T}}\{\dot{\mu}\} + \left[\frac{\partial F}{\partial A}\right]^{\mathrm{T}}\{\lambda\} + [P]^{\mathrm{T}}\{A - A_t\} = \{0\} \tag{12}$$

In addition, the boundary and terminal conditions for the Lagrange multipliers can be obtained as

$$\begin{aligned} \lambda(t_f) &= \hat{\lambda}(t_f) \quad \text{in } L \\ \mu(t_f) &= \hat{\mu}(t_f) \quad \text{in } L \\ \lambda(t) &= 0 \qquad \text{at } X_1, \quad t \in [t_0, t_f] \\ \mu(t) &= 0 \qquad \text{at } X_1, \quad t \in [t_0, t_f] \\ \lambda(t) &= 0 \qquad \text{at } X_{\mathrm{Cont.}}, \quad t \in [t_0, t_f] \end{aligned} \tag{13}$$

Moreover, the gradient of the extended performance function with respect to the control discharge can be obtained as

$$\left\{\frac{\partial J^*}{\partial Q_c}\right\} = \{s\} = -[M]^{\mathrm{T}}\{\dot{\lambda}\} + \left[\frac{\partial F}{\partial Q_c}\right]^{\mathrm{T}}\{\lambda\} + \left[\frac{\partial G}{\partial Q_c}\right]^{\mathrm{T}}\{\mu\} \tag{14}$$

2.2. Derivation of perturbation equations for state variables and Lagrange multiplier

The following perturbation equation for the state variables can be derived by the formulation that the state equation is extended by the perturbation vectors $\{Q'\}$ and $\{A'\}$ and the first-order term

DOI: 10.1002/fld

consisting of the perturbation vectors $\{Q'\}$ and $\{A'\}$ is retained:

$$[M]\{\dot{Q}'\} + \left[\frac{\partial F}{\partial Q}\right]\{Q'\} + \left[\frac{\partial F}{\partial A}\right]\{A'\} = \{0\} \tag{15}$$

$$[M]\{\dot{A}'\} + \left[\frac{\partial G}{\partial Q}\right]\{Q'\} = \{0\} \tag{16}$$

Here, the initial and boundary conditions for the perturbation equation can be denoted as

$$\begin{aligned} Q'(t_0) &= \hat{Q}'(t_0) && \text{in } L \\ A'(t_0) &= \hat{A}'(t_0) && \text{in } L \\ Q'(t) &= \hat{Q}'(t) && \text{at } X_1, \quad t \in [t_0, t_f] \\ A'(t) &= \hat{A}'(t) && \text{at } X_1, \quad t \in [t_0, t_f] \\ Q'(t) &= Q'_{\text{Cont.}}(t) && \text{at } X_{\text{Cont.}}, \quad t \in [t_0, t_f] \end{aligned} \tag{17}$$

Similarly, the following second-order adjoint equation can be obtained by the formulation that the first-order adjoint equation is extended by the perturbation vectors $\{\lambda'\}$ and $\{\mu'\}$:

$$\begin{aligned} &-[M]^{\mathrm{T}}\{\dot{\lambda}'\} + \left[\frac{\partial^2 F}{\partial Q^2}Q'\right]^{\mathrm{T}}\{\lambda\} + \left[\frac{\partial^2 G}{\partial Q^2}Q'\right]^{\mathrm{T}}\{\mu\} + \left[\frac{\partial F}{\partial Q}\right]^{\mathrm{T}}\{\lambda'\} + \left[\frac{\partial G}{\partial Q}\right]^{\mathrm{T}}\{\mu'\} \\ &\quad = \left\{\frac{\partial^2 J^*}{\partial Q_c^2}Q'_c\right\} (= \{s'\}) \end{aligned} \tag{18}$$

$$-[M]^{\mathrm{T}}\{\dot{\mu}'\} + \left[\frac{\partial^2 F}{\partial A^2}A'\right]^{\mathrm{T}}\{\lambda\} + \left[\frac{\partial F}{\partial A}\right]^{\mathrm{T}}\{\lambda'\} + [P]^{\mathrm{T}}\{A'\} = \{0\} \tag{19}$$

The above equation can be formulated based on the assumption that the following conditions are satisfied. The following conditions consist of the terms expressed by the products of the perturbations:

$$\begin{aligned} &\left[\frac{1}{2}Q'^{\mathrm{T}}\frac{\partial^3 F}{\partial Q^3}Q'\right]^{\mathrm{T}}\{\lambda\} + \left[\frac{\partial^2 F}{\partial Q^2}Q' + \frac{1}{2}Q'^{\mathrm{T}}\frac{\partial^3 F}{\partial Q^3}Q'\right]^{\mathrm{T}}\{\lambda'\} \\ &\qquad + \left[\frac{1}{2}Q'^{\mathrm{T}}\frac{\partial^3 G}{\partial Q^3}Q'\right]^{\mathrm{T}}\{\mu\} + \left[\frac{\partial^2 G}{\partial Q^2}Q' + \frac{1}{2}Q'^{\mathrm{T}}\frac{\partial^3 G}{\partial Q^3}Q'\right]^{\mathrm{T}}\{\mu'\} \\ &\quad = \left\{\frac{1}{2}Q'^{\mathrm{T}}_c\frac{\partial^3 J^*}{\partial Q_c^3}Q'_c\right\} (= \{s''\}) \end{aligned} \tag{20}$$

DOI: 10.1002/fld

$$\left[\frac{1}{2}A'^{\mathrm{T}}\frac{\partial^3 F(Q,A)}{\partial A^3}A'\right]^{\mathrm{T}}\{\lambda\}+\left[\frac{\partial^2 F(Q,A)}{\partial A^2}A'+\frac{1}{2}A'^{\mathrm{T}}\frac{\partial^3 F}{\partial A^3}A'\right]^{\mathrm{T}}\{\lambda'\}=\{0\} \tag{21}$$

Here, the terminal and boundary conditions for the second-order adjoint equation can be written as

$$\begin{aligned}
\lambda'(t_f)&=\hat{\lambda}'(t_f) \quad \text{in } L\\
\mu'(t_f)&=\hat{\mu}'(t_f) \quad \text{in } L\\
\lambda'(t)&=0 \qquad \text{at } X_1,\quad t\in[t_0,t_f]\\
\mu'(t)&=0 \qquad \text{at } X_1,\quad t\in[t_0,t_f]\\
\lambda'(t)&=0 \qquad \text{at } X_{\text{Cont.}},\quad t\in[t_0,t_f]
\end{aligned} \tag{22}$$

Finally, the traction vector given by the perturbation for the Lagrange multiplier can be calculated as

$$\begin{aligned}
\left\{\frac{\partial^2 J^*}{\partial Q_c^2}Q_c'\right\}=\{s'\}=-[M]^{\mathrm{T}}\{\dot{\lambda}'\}+\left[\frac{\partial^2 F}{\partial Q_c^2}Q_c'\right]^{\mathrm{T}}\{\lambda\}+\left[\frac{\partial^2 G}{\partial Q_c^2}Q_c'\right]^{\mathrm{T}}\{\mu\}\\
+\left[\frac{\partial F}{\partial Q_c}\right]^{\mathrm{T}}\{\lambda'\}+\left[\frac{\partial G}{\partial Q_c}\right]^{\mathrm{T}}\{\mu'\}
\end{aligned} \tag{23}$$

3. MINIMIZATION TECHNIQUE

3.1. Derivation of Newton equation

If $J(Q_{\text{Cont.}}^{(l)})$, $\{\partial J(Q_{\text{Cont.}}^{(l)})/\partial Q_{\text{Cont.}}\}$ and $[\partial^2 J(Q_{\text{Cont.}}^{(l)})/\partial Q_{\text{Cont.}}^2]$ can be obtained, $J(Q_{\text{Cont.}})$ can be approximated by Taylor expansion as

$$\begin{aligned}
J(Q_{\text{Cont.}})\fallingdotseq J(Q_{\text{Cont.}}^{(l)})+\left\{\frac{\partial J(Q_{\text{Cont.}}^{(l)})}{\partial Q_{\text{Cont.}}}\right\}^{\mathrm{T}}\{Q_{\text{Cont.}}-Q_{\text{Cont.}}^{(l)}\}\\
+\{Q_{\text{Cont.}}-Q_{\text{Cont.}}^{(l)}\}^{\mathrm{T}}\left[\frac{\partial^2 J(Q_{\text{Cont.}}^{(l)})}{\partial Q_{\text{Cont.}}^2}\right]\{Q_{\text{Cont.}}-Q_{\text{Cont.}}^{(l)}\}
\end{aligned} \tag{24}$$

It is assumed that the global minimum point for the right-hand side terms of the above equation is $Q_{\text{Cont.}}^{(l+1)}$. Therefore, the following equation can be obtained by the stationary condition:

$$\left\{\frac{\partial J(Q_{\text{Cont.}}^{(l)})}{\partial Q_{\text{Cont.}}}\right\}+\left[\frac{\partial^2 J(Q_{\text{Cont.}}^{(l)})}{\partial Q_{\text{Cont.}}^2}\right]\{Q_{\text{Cont.}}^{(l+1)}-Q_{\text{Cont.}}^{(l)}\}=\{0\} \tag{25}$$

DOI: 10.1002/fld

where $\{\partial J(Q^{(l)}_{\text{Cont.}})/\partial Q_{\text{Cont.}}\}$ and $[\partial^2 J(Q^{(l)}_{\text{Cont.}})/\partial Q^2_{\text{Cont.}}]$ are set as

$$\left\{\frac{\partial J(Q^{(l)}_{\text{Cont.}})}{\partial Q_{\text{Cont.}}}\right\} = \{g^{(l)}\} \tag{26}$$

$$\left[\frac{\partial^2 J(Q^{(l)}_{\text{Cont.}})}{\partial Q^2_{\text{Cont.}}}\right] = [H^{(l)}] \tag{27}$$

Hence, the equation for stationary condition can be expressed as

$$\{g^{(l)}\} + [H^{(l)}]\{Q^{(l+1)}_{\text{Cont.}} - Q^{(l)}_{\text{Cont.}}\} = \{0\} \tag{28}$$

where $\{g^{(l)}\}$ and $[H^{(l)}]$ refer to the steepest descent direction and Hessian matrix.

The above equation can be formulated as

$$\{Q^{(l+1)}_{\text{Cont.}}\} = \{Q^{(l)}_{\text{Cont.}}\} - [H^{(l)}]^{-1}\{g^{(l)}\} \tag{29}$$

Finally, the update equation of the control value can be obtained as follows:

$$\{Q^{(l+1)}_{\text{Cont.}}\} = \{Q^{(l)}_{\text{Cont.}}\} + \{d^{(l)}\} \tag{30}$$

where $\{d^{(l)}\}$ means the Newton direction. This direction can be calculated as

$$-[H^{(l)}]^{-1}\{g^{(l)}\} = \{d^{(l)}\} \tag{31}$$

The equation, which can be used to obtained the Newton direction, can be transformed as

$$[H^{(l)}]\{d^{(l)}\} = -\{g^{(l)}\} \tag{32}$$

which is called the Newton equation.

In addition, the control value is updated by the step length $\alpha^{(l)}$ and the Newton direction $\{d^{(l)}\}$ in the optimization problem. The update equation, which is used in the optimization problem, is expressed as

$$\{Q^{(l+1)}_{\text{Cont.}}\} = \{Q^{(l)}_{\text{Cont.}}\} + \alpha^{(l)}\{d^{(l)}\} \tag{33}$$

where the step length $\alpha^{(l)}$ is obtained by the line search algorithm. The line search algorithm is a method in which an adequate step length $\alpha^{(l)}(h)$ is obtained by gradually changing the step increment h.

3.2. Solver of the Newton equation

The Newton equation can be represented as

$$[H^{(l)}]\{d^{(l)}\} = -\{g^{(l)}\} \tag{34}$$

The conjugate gradient method is available for the solver of the Newton equation, because the Hessian matrix $[H^{(l)}]$ is a symmetric matrix. The computational algorithm of the conjugate

DOI: 10.1002/fld

gradient method is shown as follows:

1. Assume initial Newton direction $\{d_0\}$, set allowable constants ε and $l=0$. Set $\{r_0\}$ and $\{p_0\}$; $\{r_0\}=-\{g^{(l)}\}-[H^{(l)}]\{d_0\}$, $\{p_0\}=\{r_0\}$.
2. Determine α; $\alpha=\{r^{(l)}\}^{\mathrm{T}}\{r^{(l)}\}/\{p^{(l)}\}^{\mathrm{T}}[H^{(l)}]\{p^{(l)}\}$
3. Compute the Newton direction $\{d^{(l+1)}\}$; $\{d^{(l+1)}\}=\{d^{(l)}\}+\alpha^{(l)}\{p^{(l)}\}$
4. Compute the residual $\{r^{(l+1)}\}$; $\{r^{(l+1)}\}=\{r^{(l)}\}-\alpha^{(l)}[H^{(l)}]\{p^{(l)}\}$
5. Determine β; $\beta=\{r^{(l+1)}\}^{\mathrm{T}}\{r^{(l+1)}\}/\{r^{(l)}\}^{\mathrm{T}}\{r^{(l)}\}$
6. Compute the gradient $\{p^{(l+1)}\}$; $\{p^{(l+1)}\}=\{r^{(l)}\}+\beta^{(l)}\{p^{(l)}\}$
7. Check the convergence; if $\|\{d^{(l+1)}\}-\{d^{(l)}\}\|<\varepsilon$ then stop, else go to step 2.

Except the above method, the method using Lanczos tridiagonalization can also be applied to obtain the Newton direction [12–14].

3.3. BFGS method

The DFP method (Davidon–Fletcher–Powell method) [15] and the BFGS method (Broyden–Fletcher–Goldfarb–Shanno method) [16], which are formulated by the secant equation [17], are methodologies used to obtain a Hessian matrix. These methods ensure that the Hessian matrix is positive definite and symmetrical. These methods are therefore frequently used to calculate the Hessian matrix.

In this study, the BFGS method is applied to obtain the Hessian matrix. The update equation of Hessian matrix by using the BFGS method can be written as

$$[H^{(l+1)}]=[H^{(l)}]+\frac{\{g'^k\}\{g'^k\}^{\mathrm{T}}}{\{g'^k\}^{\mathrm{T}}\{Q'^k_{\mathrm{Cont.}}\}}-\frac{[H^{(l)}]\{Q'^k_{\mathrm{Cont.}}\}\{Q^{k\prime}_{\mathrm{Cont.}}\}^{\mathrm{T}}[H^{(l)}]}{\{Q'^k_{\mathrm{Cont.}}\}^{\mathrm{T}}[H^{(l)}]\{Q'^k_{\mathrm{Cont.}}\}} \tag{35}$$

where $\{Q'_{\mathrm{Cont.}}\}$, $\{g'\}$ and $\{s'\}$ are denoted as

$$\begin{aligned}[H^{(l)}]&=\left[\frac{\partial^2 J^{*(l)}}{\partial Q^2_{\mathrm{Cont.}}}\right]\\ \{Q'^k_{\mathrm{Cont.}}\}&=\{Q^{(l+1)}_{\mathrm{Cont.}}\}-\{Q^{(l)}_{\mathrm{Cont.}}\}\\ \{g'^k\}&=\left\{\frac{\partial J^{*(l+1)}}{\partial Q^k_{\mathrm{Cont.}}}\right\}-\left\{\frac{\partial J^{*(l)}}{\partial Q^k_{\mathrm{Cont.}}}\right\}=\{g^{(l+1)}\}-\{g^{(l)}\}\end{aligned} \tag{36}$$

Here, $\{s'\}$, which means the traction vector given by the perturbation for the Lagrange multiplier, can be shown as

$$\{s'^{(l)}\}=[H^{(l)}]\{Q'^k_{\mathrm{Cont.}}\}=\left[\frac{\partial^2 J^{*(l)}}{\partial Q^2_{\mathrm{Cont.}}}\right]\{Q'^k_{\mathrm{Cont.}}\} \tag{37}$$

Consequently, the update equation of the Hessian matrix can be represented as

$$[H^{(l+1)}]=[H^{(l)}]+\frac{\{g'^k\}\{g'^k\}^{\mathrm{T}}}{\{g'^k\}^{\mathrm{T}}\{Q'^k_{\mathrm{Cont.}}\}}-\frac{\{s'^{(l)}\}\{s'^{(l)}\}^{\mathrm{T}}}{\{Q'^k_{\mathrm{Cont.}}\}^{\mathrm{T}}\{s'^{(l)}\}} \tag{38}$$

DOI: 10.1002/fld

In general, the product of the Hessian matrix $[H]$ and the perturbation $\{Q'_{\text{Cont.}}\}$ cannot be obtained directly. Conventionally, this product is calculated by using an approximated Hessian matrix. However, the traction given by the perturbation for the Lagrange multiplier expressed by exact Hessian matrix can be obtained using this approach. Therefore, it is considered that a more exact Newton direction can be obtained than with conventional method [10].

3.4. Newton-based method

The computational algorithm of the Newton-based method is similar to the gradient methods such as, the Fletcher–Reeves method, the weighted residual method, the conjugate direction method, the steepest descent method and so on. The difference between the Newton-based method and the gradient-based methods is the descent direction that is used for the update equation of the control variables. In the gradient methods, the steepest descent direction is used directly for the update equation of control variables. On the other hand, in the Newton-based method, the Newton direction which is obtained by the steepest descent direction is used for the update equation of control variables. The computational algorithm is shown below.

1. Choose an initial control value $\{Q^{(l)}_{\text{Cont.}}\}$, an initial Hessian Matrix $[H^{(l)}]$ and a convergence criterion ε.
2. Compute the state value $\{Q^{(l)}\}$, $\{A^{(l)}\}$ using the state equation.
3. Compute the performance function $J^{(l)}$.
4. Compute the Lagrange multiplier $\{\lambda^{(l)}\}$, $\{\mu^{(l)}\}$ and the steepest descent direction $\{g^{(l)}\}$.
5. Solve the Newton equation $[H^{(l)}]\{d^{(l)}\} = -\{g^{(l)}\}$ using the conjugate gradient method.
6. Generate a new control value $\{Q^{(l+1)}_{\text{Cont.}}\}$ by the Newton direction $\{d^{(l+1)}\}$ and the step length $\alpha^{(l+1)}$.
7. Compute the state value $\{Q^{(l+1)}\}$, $\{A^{(l+1)}\}$ by the state equation.
8. Compute the performance function $J^{(l+1)}$.
9. Compute the Lagrange multiplier $\{\lambda^{(l+1)}\}$, $\{\mu^{(l)}\}$ and the steepest descent direction $\{g^{(l+1)}\}$.
10. Check the convergence: if $\|\{Q^{(l+1)}_{\text{Cont.}}\} - \{Q^{(l)}_{\text{Cont.}}\}\| < \varepsilon$ then stop, else go to step 11.
11. Compute the perturbed solution $\{Q'^{(l+1)}\}$, $\{A'^{(l+1)}\}$ using the perturbation equation for state variables.
12. Compute the Lagrange multiplier $\{\lambda'^{(l+1)}\}$, $\{\mu'^{(l+1)}\}$ and the traction given by the perturbation for the Lagrange multiplier $\{s'^{(l+1)}\}$.
13. Compute the Hessian matrix $[H^{(l+1)}]$ by the $\{Q^{(l+1)}_{\text{Cont.}}\} - \{Q^{(l)}_{\text{Cont.}}\}$, $\{g^{(l+1)}\} - \{g^{(l)}\}$ and $\{s'^{(l)}\}$.
14. Solve the Newton equation $[H^{(l+1)}]\{d^{(l+1)}\} = -\{g^{(l+1)}\}$ using the conjugate gradient method and go to 6.

The initial Hessian matrix is generally set as a unit matrix.

4. NUMERICAL EXPERIMENTS

4.1. Verification of computational algorithm by second-order adjoint technique

A simple conduit flow problem is used as a numerical study. The diagram of this study is illustrated in Figure 3. The length of conduit is 20 m and the observation point is set at the point A. The total points of node and element are, respectively, 200 and 199. The slope of conduit is set 0.5%.

DOI: 10.1002/fld

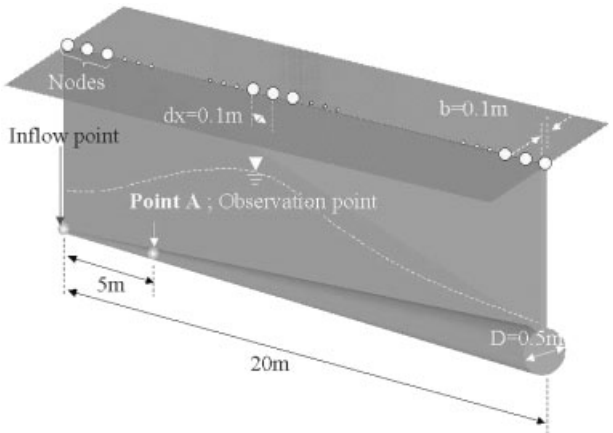

Figure 3. Computational model and finite-element division.

Table I. Computational conditions.

Number of time steps	10 000
Time increment Δt (s)	0.001
Manning coefficient of roughness n (s/m$^{1/3}$)	0.013

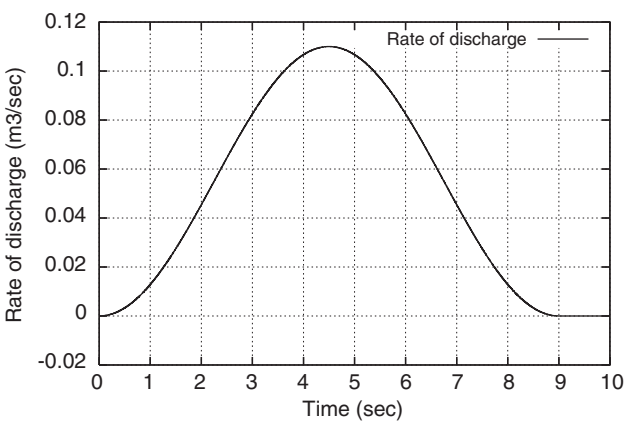

Figure 4. Time history of rate of discharge.

The computational conditions for this analysis are listed in Table I. The values of the weighting diagonal matrix $[P]$ at the target point are 1.0 and those at other points are 0.0.

In case that the flow shown in Figure 4 is given from the upstream side of conduit, the time history of water level shown in Figure 5 can be obtained as the computational result. Here, let

DOI: 10.1002/fld

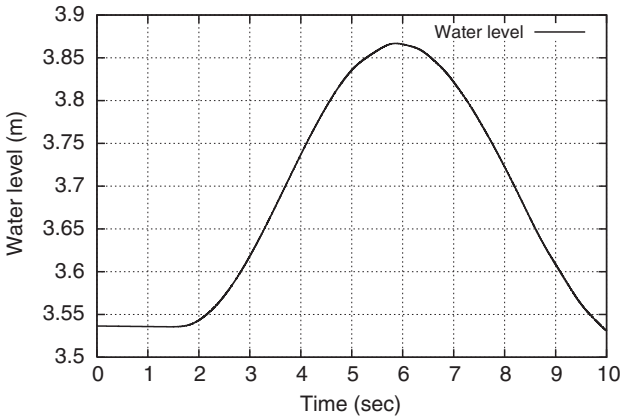

Figure 5. Time history of water level at observation point.

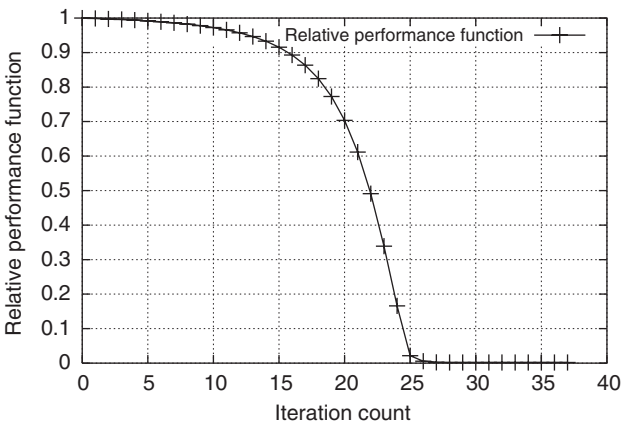

Figure 6. Convergence history of performance function.

us consider the problem that we have the time history of the water level shown in Figure 5 and would like to know the time history of the rate of discharge at the inflow point. The purpose of this study is to find the rate of discharge such that the computed water level is in good agreement with the observed water level.

4.1.1. Computational results by first-order adjoint technique. This section discusses the problem when the gradient method is applied to this study. The computational results are shown in Figures 6–8. Figure 6 shows the convergence history of the performance function. The performance function gradually decreases and finally converges. Consequently, the water level at the observation point is in good agreement with the observed water level as shown in Figure 7, and

DOI: 10.1002/fld

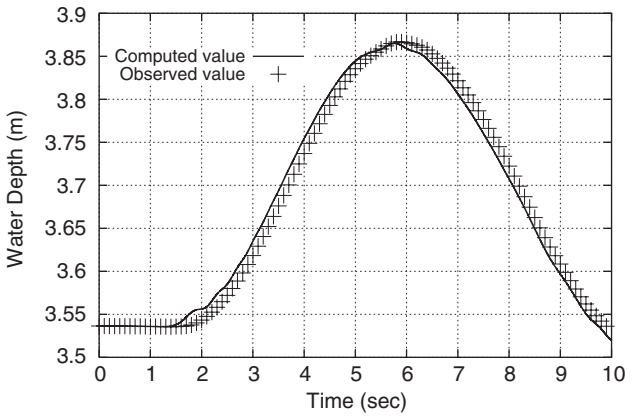

Figure 7. Comparison between computed water level and assumed water level.

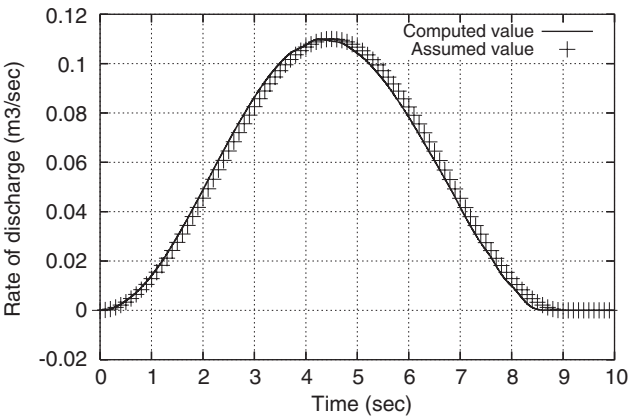

Figure 8. Comparison between computed value and assumed rate of discharge.

the rate of discharge can be obtained as shown in Figure 8. It is found that the computed value is also in good agreement with the assumed rate of discharge.

4.1.2. Computational results by second-order adjoint technique. This section discusses the computational results obtained by the second-order adjoint technique. The computational results are shown in Figures 9–11. Figure 9 shows the convergence history of the performance function. The performance function gradually decreases and finally converges. The fast convergence rate can be obtained in comparison with the case that the gradient method is applied. Consequently, the water level at the observation point is in good agreement with the observed water level as shown in Figure 10, and the rate of discharge can be obtained as shown in Figure 11. It is found that the computed value is also in good agreement with the assumed rate of discharge as well as the result

DOI: 10.1002/fld

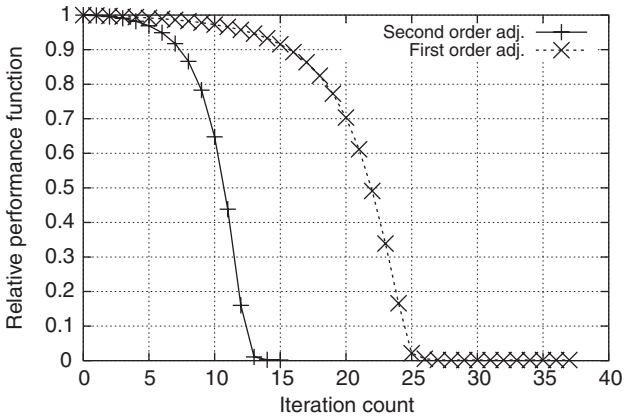

Figure 9. Convergence history of the performance function.

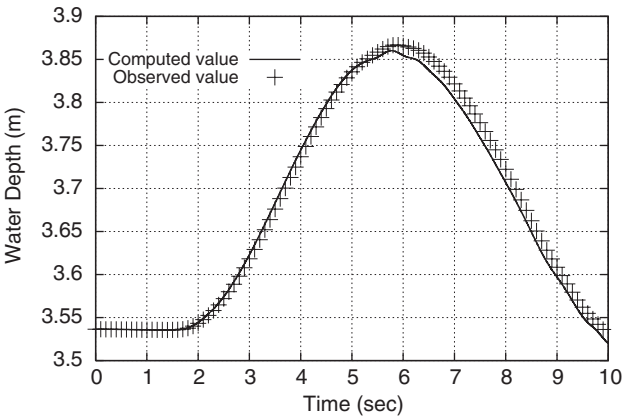

Figure 10. Comparison between computed water level and assumed water level.

of the gradient method. In addition, the comparison of computational time between the first-order adjoint technique and the second-order adjoint technique is shown in Table II. The computational time could be reduced by 28% than with that of the first-order adjoint technique.

4.2. Application to flood control problem

In this section, the second-order adjoint technique is applied to a flood control problem. Here, an urban area shown in Figure 12 is used as an example of practical problem. Figure 12 shows the aerophotograph in the examination area and the flood expectation district. It is said that the flood will occur at the area shown in the photograph in case of heavy rainfall that the rainfall intensity is 50 mm/h. Therefore, a countermeasure that the stormwater tunnel reservoir will be constructed

DOI: 10.1002/fld

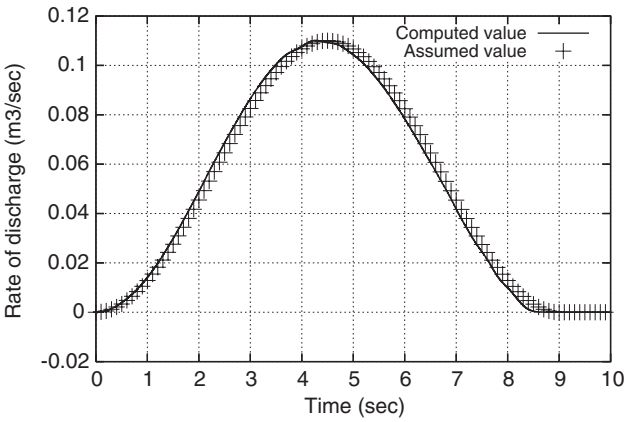

Figure 11. Comparison between computed value and assumed rate of discharge.

Table II. Comparison of computational time.

First-order adjoint technique	28 min 25 s
Second-order adjoint technique	20 min 25 s

Figure 12. Flood expectation district.

in the underground is considered by the local authority. Thus, the purpose of this study is to find the adequate control discharge to the stormwater reservoir so as to prevent the flood damage. Figures 13 and 14 show the boundary line for the each catchment districts in the examination area and the diagram of conduits network. To compute the flow behaviour, the conduits network is divided into 2565 elements. The total points of nodes are 2566. The inflow boundary conditions,

DOI: 10.1002/fld

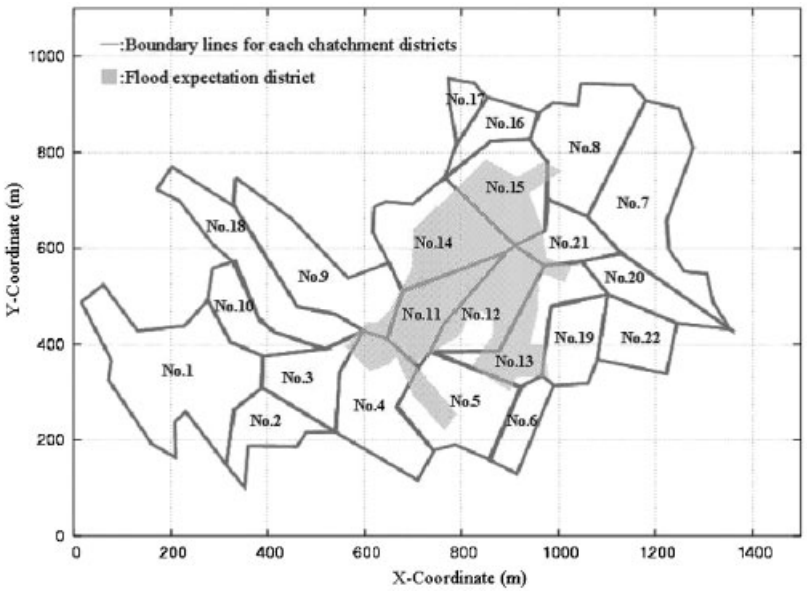

Figure 13. Boundary lines for each catchment district.

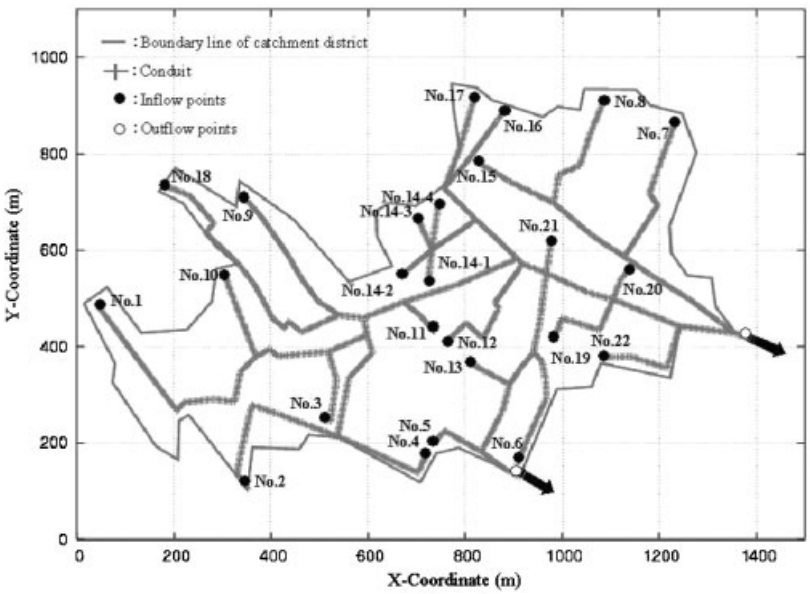

Figure 14. Diagram of conduits network.

DOI: 10.1002/fld

Table III. Areas for each catchment district.

Number	Area (ha)
No. 1	6.69
No. 2	1.76
No. 3	2.02
No. 4	3.52
No. 5	3.44
No. 6	1.20
No. 7	5.05
No. 8	3.80
No. 9	3.99
No. 10	1.70
No. 11	1.98
No. 12	2.42
No. 13	3.40
No. 14	3.76
No. 15	2.94
No. 16	1.24
No. 17	0.59
No. 18	4.23
No. 19	1.85
No. 20	1.69
No. 21	1.48
No. 22	1.77
—	—
Total	60.50

which mean the rainfall conditions, are given at the starting points of conduits in each catchment district. The inflow boundary condition is frequently calculated by the rational equation

$$Q_{\text{inflow}} = \tfrac{1}{360} CIA \tag{39}$$

Here, Q_{inflow}, C, I and A mean the rate of discharge at inflow point, the runoff coefficient, the rainfall intensity and the catchment area. The areas for each catchment districts are shown in Table III and the time history of the rainfall intensity is shown in Figure 15. This time history of rainfall intensity means the rainfall of 50 mm/h. In addition, the runoff coefficient is set 0.8 and the other computational conditions are shown in Table IV. In addition, the values of the weighting matrix $[P]$ at the target points are 1.0 and those at other points are 0.0.

In the flood expectation district, the target points are set to two points in the main conduit. Additionally, the control points are set two points over the stormwater tunnel reservoir. The location of the target and control points is shown in Figure 16.

The purpose of this study is to obtain the adequate control discharge at the control points such that the water level at the target points reduce to the target water level. The target water level is set as the initial water level 1.0 m.

As the computational results, the variation of performance function is shown in Figure 17. The value of the performance function monotonously decreases and finally converges. Consequently, the adequate control discharge shown in Figures 18 and 19 could be obtained. Figures 18 and 19 denote the time histories of the control discharge at the control points Nos 1 and 2. In addition,

DOI: 10.1002/fld

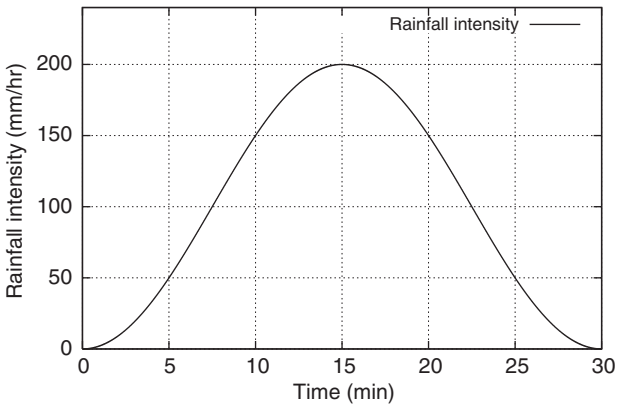

Figure 15. Time history of rainfall intensity.

Table IV. Computational conditions.

Number of time steps	3600
Time increment Δt (s)	0.50
Manning coefficient of roughness n (s/m$^{1/3}$)	0.013
Runoff coefficient C	0.80

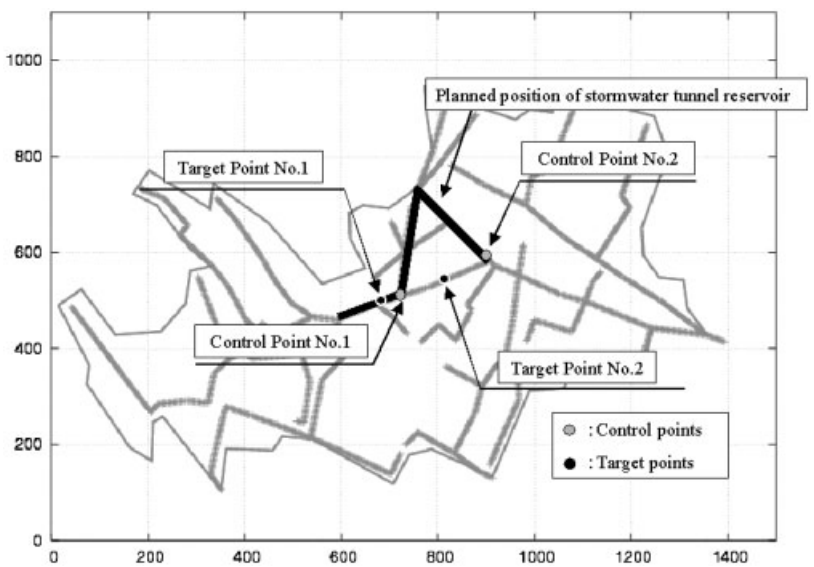

Figure 16. Location of target and control points.

DOI: 10.1002/fld

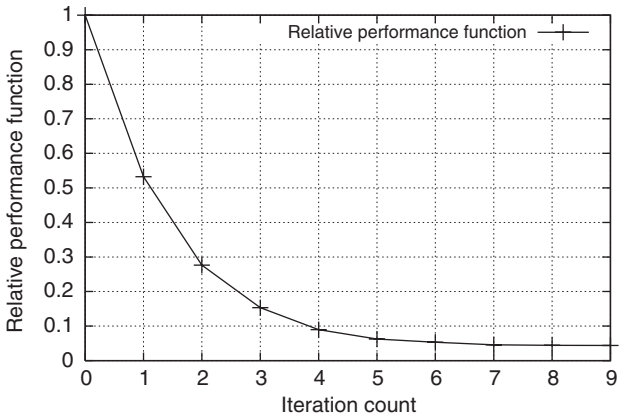

Figure 17. Convergence history of performance function.

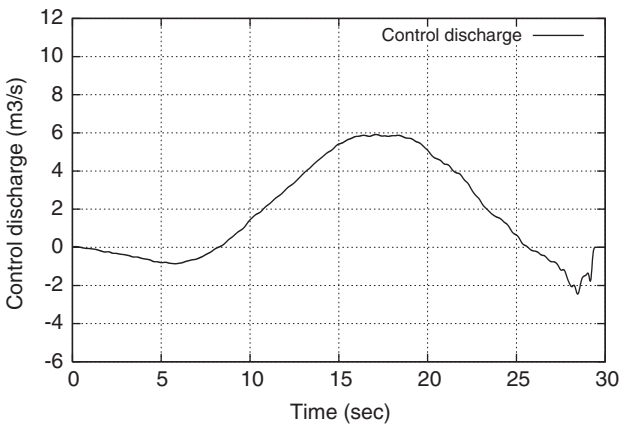

Figure 18. Time history of control discharge at control point No. 1.

the time history of water level at the target points Nos 1 and 2 is shown in Figures 20 and 21. The solid line means the water level with control case and the broken line means the water level without control case. At the target points Nos 1 and 2, the water level could be reduced to the target water level by giving the adequate control discharge.

5. CONCLUSIONS

In this paper, the second-order adjoint technique was applied to the inverse problems for conduit flow. As state equations, the Saint–Venant equation was employed to express the flow behaviour. The Galerkin method using the bubble function element and the Crank–Nicolson method, respectively,

DOI: 10.1002/fld

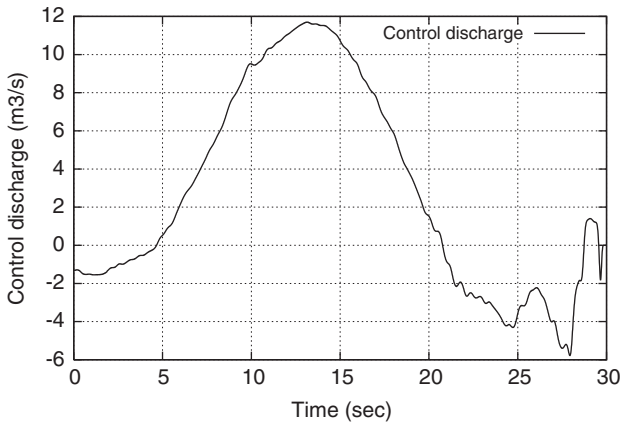

Figure 19. Time history of control discharge at control point No. 2.

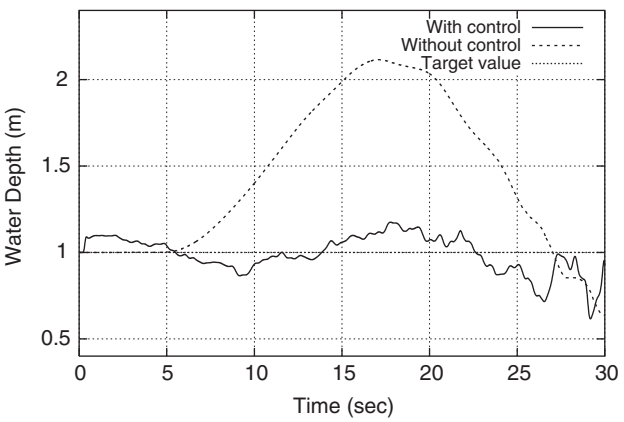

Figure 20. Time history of water level at target point No. 1.

were used for the spatial and temporal discretizations. The Newton-based method by the BFGS method using the traction given by the perturbation for the Lagrange multiplier is used as the minimization technique. As the numerical examples, the estimation problem of rate of discharge and the flood control problem were used. The conclusions of this study are written as follows:

- The propriety of the second-order adjoint technique for the conduit flow problem could be confirmed.
- In case that the Newton-based method was employed, the fast convergence rate could be confirmed.
- In the verification problem, the computational time could be reduced by 28% in comparison with that of the first-order adjoint technique.

DOI: 10.1002/fld

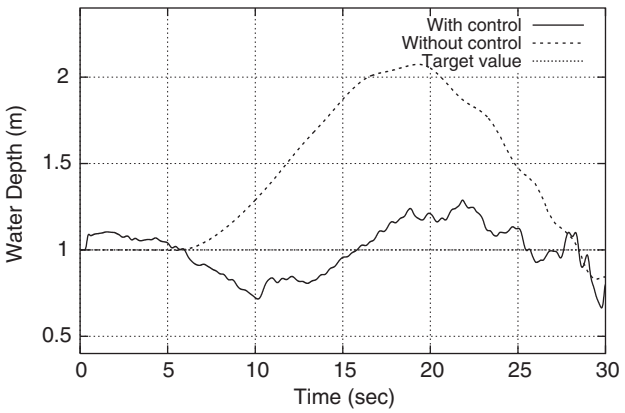

Figure 21. Time history of water level at target point No. 2.

- In the flood control problem, the adequate control discharge could be obtained by the second-order adjoint technique.

For the future, it is desired that this methodology be applied to the other boundary value determination problems.

REFERENCES

1. Quintana VH, Davidon EJ. Clipping-off gradient algorithms to compute optimal controls with constrained magnitude. *International Journal of Control* 1974; **20**(2):243–255.
2. Sakawa Y, Shindo Y. On global convergence of an algorithm for optimal control. *IEEE Transactions on Automatic Control* 1980; **ac-25**(6):1149–1153.
3. Navon IM, Brown FB, Robertson DH. A combined simulated annealing and quasi-Newton-like conjugate-gradient method for determining the structure of mixed Argon–Xenon clusters. *Computers and Chemistry* 1990; **14**:305–311.
4. Zou X, Navon IM, Berger M, Phua KH, Schlick T, Le Dimet FX. Numerical experience with limited-memory quasi-Newton and truncated Newton methods. *SIAM Journal on Optimization* 1993; **3**(3):582–608.
5. Morales JL, Nocedal J. Automatic preconditioning by limited memory quasi-Newton updating. *SIAM Journal on Optimization* 2000; **10**(4):1079–1096.
6. Wang Z, Navon IM, Zou X, Le Dimet FX. A truncated Newton optimization algorithm in meteorology applications with analytic Hessian/vector products. *Computational Optimization and Applications* 1995; **4**:241–262.
7. Alekseev AK, Navon IM. On estimation of temperature uncertainty using the second order adjoint problem. *International Journal of Computational Fluid Dynamics* 2002; **16**(2):113–117.
8. Alekseev AK, Navon IM. Calculation of uncertainty propagation using adjoint equations. *International Journal of Computational Fluid Dynamics* 2003; **17**(4):283–288.
9. Wang Z, Navon IM, Le Dimet FX, Zou X. The second order adjoint analysis: theory and applications. *Meteorology and Atmospheric Physics* 1992; **50**:3–20.
10. Kurahashi T, Kawahara M. Development of second-order adjoint technique for boundary value determination problems. *International Journal for Numerical Methods in Engineering*, submitted.
11. Chaudhry MH. *Applied Hydraulic Transients*. Van Nostrand Reinhold: New York, 1987; 422–423.
12. Nash SG. Preconditioning of truncated-Newton methods. *SIAM Journal on Scientific and Statistical Computing* 1985; **6**(3):599–616.
13. Nash SG. Newton-type minimization via the Lanczos method. *SIAM Journal on Numerical Analysis* 1984; **21**(4):770–788.

DOI: 10.1002/fld

14. Nash SG, Sofer A. Preconditioning reduced matrices. *SIAM Journal on Matrix Analysis and Applications* 1996; **17**(1):47–68.
15. Fletcher R, Powell MJD. A rapidly convergent descent method for minimization. *Computer Journal* 1963; **6**:163–168.
16. Fletcher R. A new approach to variable metric algorithms. *Computer Journal* 1970; **13**:317–322.
17. Dennis Jr JE, Schnabel RB. Least change secant updates for quasi Newton methods. *SIAM Review* 1979; **21**:443–459.

DOI: 10.1002/fld